Experimental Physiology

Using Physiome standards to couple cellular functions for rat cardiac excitation–contraction

Jonna R. Terkildsen[1], Steven Niederer[2], Edmund J. Crampin[1,3], Peter Hunter[1] and Nicolas P. Smith[2]

[1]*Auckland Bioengineering Institute and* [3]*Department of Engineering Science, University of Auckland, Auckland, New Zealand*
[2]*Computing Laboratory, University of Oxford, Oxford, UK*

Scientific endeavour is reliant upon the extension and reuse of previous knowledge. The formalization of this process for computational modelling is facilitated by the use of accepted standards with which to describe and simulate models, ensuring consistency between the models and thus reducing the development and propagation of errors. CellML 1.1, an XML-based programming language, has been designed as a modelling standard which, by virtue of its import and grouping functions, facilitates model combination and reuse. Using CellML 1.1, we demonstrate the process of formalized model reuse by combining three separate models of rat cardiomyocyte function (an electrophysiology model, a model of cellular calcium dynamics and a mechanics model) which together make up the Pandit–Hinch–Niederer *et al.* cell model. Not only is this integrative model of rat electromechanics a useful tool for cardiac modelling but it is also an ideal framework with which to demonstrate both the power of model reuse and the challenges associated with this process. We highlight and classify a number of these issues associated with combining models and provide some suggested solutions.

(Received 19 December 2007; accepted after revision 4 March 2008; first published online 14 March 2008)
Corresponding author N. P. Smith: Computing Laboratory, University of Oxford, Oxford OX1 3QD, UK.
Email: nic.smith@comlab.ox.ac.uk

As experimental tools have become increasingly sophisticated, the ability to assay biological function across a range of spatial scales has given rise to an abundance of biological data extending from genomic description up to whole-organ function. The challenge facing researchers today is to determine how this information can be unified to improve understanding of normal and pathological physiology. Mathematical modelling is a powerful technique to apply to this challenge. Using these comprehensive experimental datasets, accurate biophysical, multi-scale computational models may be constructed to investigate, for example, the influence of subcellular changes upon whole-organ function.

However, systems biology, like all scientific endeavours, is intrinsically dependent upon the reuse of current knowledge as building blocks. As models develop in complexity, it is becoming increasingly important to build upon models that have been developed in the past. Through the careful amalgamation of component models (each providing a functional description of a single biological process), it is possible to generate biological complexity in a straightforward and reliable manner. This concept of modularity may be applied to any spatial scale such that, with thorough analysis, large-scale models of biological systems may be developed in an incremental fashion. Thus, this systems biology-type approach facilitates insights into a specific biological problem without the labour-intensive process of model development from scratch.

In order to achieve this information reuse in a modelling environment, it is necessary to have a consistent means for representing these systems, thus facilitating reliable reuse of components. Such a standard would need to be a means with which one may represent these models mathematically (thus avoiding misrepresentations common in publications), as well as provide a mechanism for coupling individual models (thus alleviating incompatibility issues associated with different programming languages or modelling environments).

CellML 1.1, designed as a modelling language with these objectives in mind, is an XML-based language that uses MathML to represent the mathematics of a model in a manner which is both human- and computer-readable (Lloyd *et al.* 2004). The component nature of this modelling environment means that small, individual

 DOI: 10.1113/expphysiol.2007.041871

biological entities are encoded as component models and are combined to formulate a complete model. Additional structure, both physical and conceptual, is introduced to the model through the use of grouping relationships between components. Furthermore, CellML 1.1 has the ability to import individual components from other models, facilitating the reuse and integration of models (Cuellar *et al.* 2003).

The combination of these features (component nature, grouping and importation functions), means that CellML 1.1 is an ideal tool to underpin a systems biology approach at a cellular spatial scale, whereby smaller models may be designed and validated separately, and combined into an ensemble model representing increased function and/or physiological complexity.

While the potential of being able to couple independently developed models is clear (Hunter & Borg, 2003), few examples of this exist in the literature and none, to our knowledge, provides a transparent methodology for how this may be achieved. This paper aims to demonstrate the model reuse capabilities of CellML 1.1, using cardiac electrophysiology modelling as an example of computational modelling which is not only highly developed but also has a strong link to the experimental data. More specifically, we will demonstrate how three separate models of rat cardiomyocyte function [namely, an electrophysiology model (Pandit *et al.* 2001), a model of calcium dynamics (Hinch *et al.* 2004) and a mechanics model (Niederer *et al.* 2006), as per our previous study (Niederer & Smith, 2007)] may usefully be combined. Thus this paper serves a dual purpose: to demonstrate the power of model reuse and how this may be achieved in CellML and, furthermore, to make available an integrative model of rat electrophysiology and active contraction, a useful tool for further study of cardiac physiology.

Lastly, while the reuse and elaboration of existing models provides an exciting development path for computational biology, care must be taken in the process such that correct parameter values and modelling structure is maintained. The introduction of a standard, such as CellML, will greatly alleviate this problem (especially if a version of the model in CellML, or another commonly used language, is added to the online repository concurrent with the publishing of the model), although care must still be exercised in the reuse of CellML components. We will highlight indicative examples of each type of challenge which may be encountered during this process, along with suggested solutions.

Methodology

We have previously developed a comprehensive model of adult rat cardiomyocyte electromechanical function (Niederer & Smith, 2007) to investigate the slow force response to stretch. The 'core' cell model (upon which the slow force response was built) couples a description of rat electrophysiology in endocardial ventricular myocytes (as presented by Pandit *et al.* 2001) with our model of active contraction in rat cardiomyocytes (Niederer *et al.* 2006). These two models are linked by Hinch and co-workers' novel model of Ca^{2+} dynamics (Hinch *et al.* 2004).

This core model, hereafter termed the Pandit–Hinch–Niederer *et al.* (PHN *et al.*) model, is an ideal framework to demonstrate the application of model reuse. In the previous study (Niederer & Smith, 2007), the component models were combined through the recoding (and adaptation) of their model equations or parts thereof. In contrast, in the present study we demonstrate how the core model may be constructed by coupling the aforementioned component models without further modification to their original mathematical and computational formulations.

The individual models were separately represented in CellML (available in the online CellML repository, http://www.cellml.org/models), and verified against the original publication images, before being used to create the PHN *et al.* model. In each case, the models were integrated using the CellML editor and integrator, PCEnv (http://www.cellml.org/tools/pcenv), using the inbuilt Adams–Moulton integration algorithm (a variable order, variable time step size integration algorithm with internal error checking) with a maximal time step size of 1.0 ms and error tolerances of 1.0×10^{-6} to bound the error between the integration and true solutions.

The encoding and curation of these models in CellML highlights the types of typographical errors which are common in the publication of computational models. That is, the misrepresentation or omission of model equations, parameters or state variable initial conditions from the published format. As demonstrated below, none of the component models used in this study is free of these typographical errors, and the corrected equations and initial conditions are included in the Appendix. A brief description of each of these constituent models and their formulation in CellML is presented below.

Finally, the formulation of the PHN *et al.* model will be described, along with a description of the process of model coupling and associated issues.

Pandit model of rat cardiomyocyte electrophysiology

The Pandit model of rat cardiomyocyte electrophysiology characterizes the major currents and cellular features contributing to the development of the sarcolemmal action potential (AP) waveform in both epicardial and endocardial cells of the left ventricle (Fig. 1*A*).

Model curation. The mathematical formulations of the fast Na^+ channel gating, the L-type Ca^{2+} channel gating, the inward rectifier channel and the Na^+–K^+ pump,

as described in the paper, do not precisely conform to the mathematics of the referenced models (S. V. Pandit, personal communication). Thus, the model equations were modified accordingly (details in the Appendix).

The voltage dependence of the fast Na^+ channel gating variables (using the updated equations), in comparison to that of the original publication (Pandit *et al.* 2001), is shown in Fig. 2.

Model verification. Once a model has been encoded in CellML, it is important to verify that it accurately represents the mathematics of the authors and is able to reproduce publication results. To verify the CellML implementation of the Pandit electrophysiology model, both the epicardial and the endocardial cell models were stimulated with a 5 ms stimulus current of amplitude 0.6 nA. The comparison between the resultant action potential waveforms and those of Fig. 8 of Pandit *et al.* (2001) is shown in Fig. 3. Table 1 presents a numerical comparison of the main characteristics of the action potentials. As is evident in this table, there are slight discrepancies between the computed values from the CellML model and those listed in the paper. These may stem from variabilities in the integration parameters (such as choice of integrator, maximal step size, etc.) or algorithm (this study used the Adams–Moulton integration algorithm, in contrast to the Runge–Kutta–Mersen integration algorithm used by Pandit and co-workers).

Although this model presents a well-developed framework which may be used as a basis for the incorporation of additional data, Pandit and his co-workers acknowledge that the model has one significant limitation, namely the calcium handling in

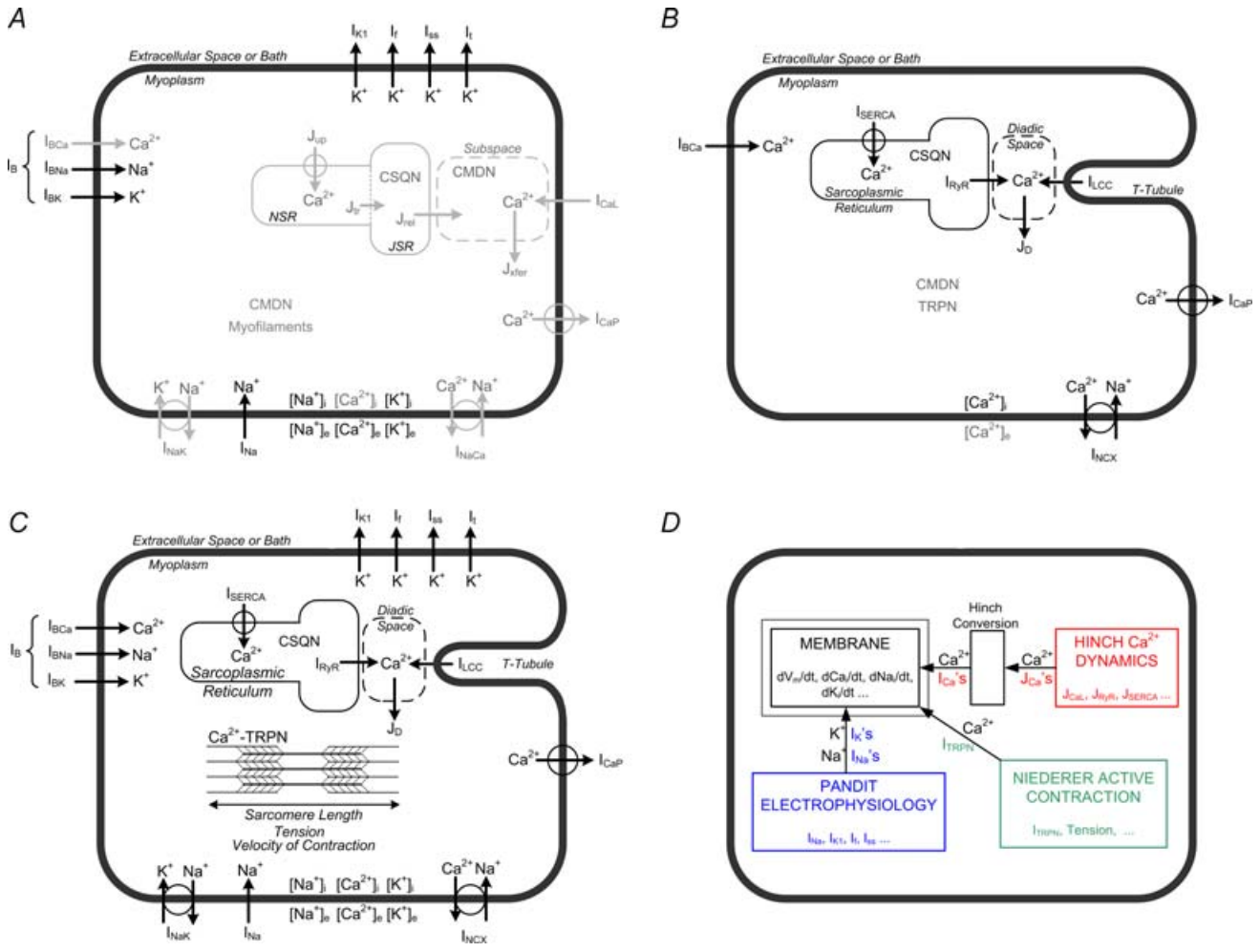

Figure 1. Schematic diagram of cell models
A, Pandit *et al.* cell model. *B*, Hinch *et al.* model of Ca^{2+} dynamics. Bold lines represent components which are imported into the PHN *et al.* cell model, and grey lines indicate components which are not imported into the PHN *et al.* model. *C*, PHN *et al.* cell model. *D*, schematic diagram of the structure of the PHN *et al.* cell model. Abbreviations: PHN, Pandit-Hinch-Niederer.

the sarcoplasmic reticulum. For this reason, the cellular calcium handling in the PHN *et al.* model was replaced by that of Hinch *et al.* (2004), described in the following subsection.

Hinch model of calcium dynamics

Hinch and colleagues formulated a comprehensive model of rat cardiomyocyte Ca^{2+} dynamics with the primary aim of creating a computationally efficient (local control) model of calcium-induced calcium release. This 'coupled LCC–ryanodyne receptor (RyR) gating model' assumes that a calcium release unit (CaRU) consists of one L-type Ca^{2+} channel, one RyR channel and the dyadic subspace between the T-tubules and the sarcoplasmic reticulum (SR) into which they both transport Ca^{2+} ions. Notably, these authors have created a model of graded Ca^{2+} release from the SR in ordinary differential equation (ODE) format, thus converting a stochastic model of Ca^{2+} handling to a computationally efficient ODE model. This model further includes descriptions of sarcolemmal and sarcoplasmic reticulum Ca^{2+} channels, as well as calmodulin and calsequestrin Ca^{2+} buffering, thus representing complete cellular Ca^{2+} dynamics (see Fig. 1*B*).

Model curation. The published form of the Hinch model also contains typographical errors. In this case, there is uncertainty regarding the mathematical formulation of the sodium–calcium exchange current, in addition to the omission of the initial conditions of some state variables. The details of those used in this CellML representation are listed in the Appendix.

Model verification. To verify this CellML implementation, a voltage-step depolarization (from −80 to 0 mV for 200 ms) was simulated as in Fig. 7 of Hinch *et al.* (2004). Figure 4 shows the simulated results against a reproduction of the original figure. Figure 5 shows the voltage dependence of both the L-type Ca^{2+} channel and the RyR release channel, as in the original Fig. 8a.

Niederer model of active contraction

Using the framework of Hunter *et al.* (1998), we have previously formulated a model of active contraction of the ventricular myocyte (Niederer *et al.* 2006). The model represents Ca^{2+} binding to troponin C, tropomyosin and cross-bridge kinetics. The effects of the multiple length, velocity and tension feedback mechanisms that regulate tension development in the heart are explicitly represented in the model. The model parameters were determined by an extensive review of the literature and chosen to best reflect tension development in rat cardiac myocytes at room temperature. The final model was demonstrated to replicate quantitatively a broad range of

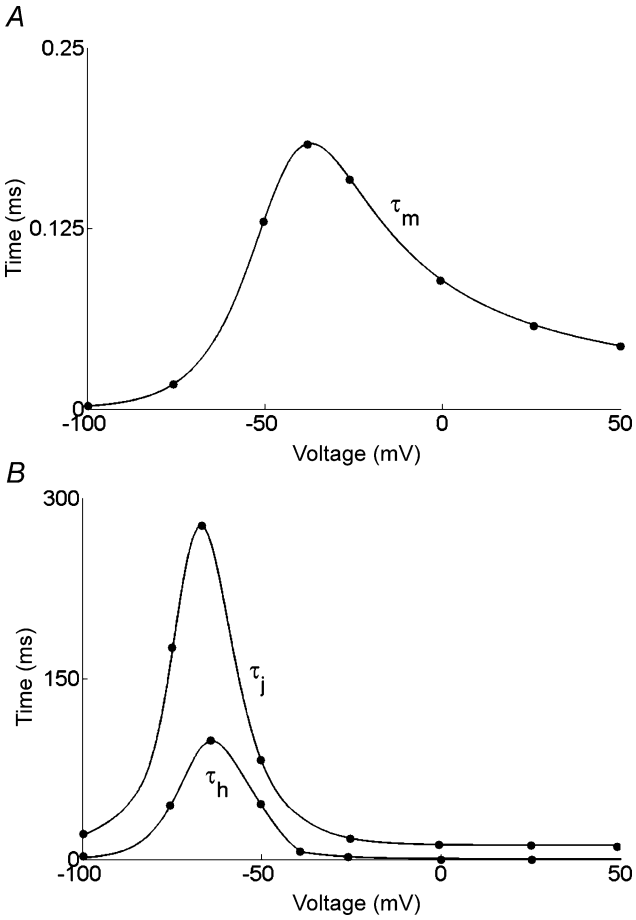

Figure 2. Pandit fast Na^+ channel activation and inactivation time constants
Pandit fast Na^+ channel activation time constant (τ_m; *A*) and inactivation time constants (τ_j and τ_h; *B*) predicted by the CellML model (continuous line) against digitized data (dots) from Fig. 2 Pandit *et al.* (2001).

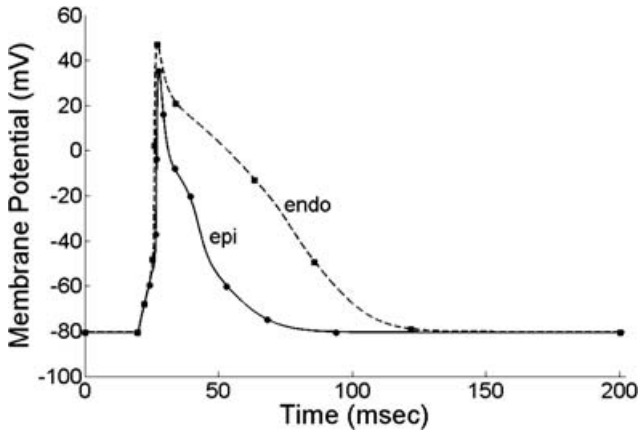

Figure 3. Verification of the Pandit CellML implementation
Epicardial (continuous line) and endocardial action potential waveforms (dashed line) predicted by the CellML model against digitized data (dots) from Fig. 8 of Pandit *et al.* (2001).

Table 1. Verification of the Pandit Model CellML implementation

	Epicardial model		Endocardial model	
	Original paper	CellML model	Original paper	CellML model
V_{rest} (mV)	−80.44	−80.5	−80.37	−80.35
Peak overshoot (mV)	35.75	35.67	47.08	46.0
APD_{90} (ms)	39.68	40.83	76.43	76.5

V_{rest}, resting membrane potential; APD_{90}, action potential duration at 90% repolarization.

experimental results, including: tension changes following instantaneous increases and decreases in free Ca^{2+}; steady-state force–Ca^{2+} relationship; muscle dynamic stiffness; and step changes in muscle length.

Model curation. The published version of this model is also not free of typographical errors. The equation representing z_{max} (the fraction of actin sites available at maximum activation) is incorrect and was replaced by eqn (A10) of the Appendix.

Model verification. To verify the correct implementation of the Niederer active contraction model, we replicated Fig. 11a from Niederer *et al.* (2006) by calculating the tension response to a calcium stimulus transient (data from Fig. 1c of Janssen *et al.* 2002; 22.5°C trace) for increasing values of sarcomere length [λ (equal to the ratio of sarcomere length divided by the resting sarcomere length of 2 μm) ranging from 1.8 to 2.2 μm; Fig. 6].

Pandit–Hinch–Niederer *et al.* (PHN *et al.*) model

Using the three individual models just described, a single model of the rat ventricular cardiomyocyte was created. The sarcolemmal Na^+ and K^+ currents described by the Pandit *et al.* endocardial model were combined with the description of cellular Ca^{2+} fluxes from Hinch *et al.*, whilst the mechanisms of Ca^{2+} binding to troponin C and the associated tension development (active contraction) was characterized by Niederer *et al*. The CellML 1.1 code for the PHN *et al.* model is available from the online CellML 1.1 repository (www.cellml.org/models_1.1). Figure 1*C* shows a schematic diagram of the PHN *et al.* model which is constructed from the imported components shown in bold in the schematic diagrams of the Pandit and Hinch models (Fig. 1*A* and *B*) in addition to the Niederer active contraction model. The structure of the composite

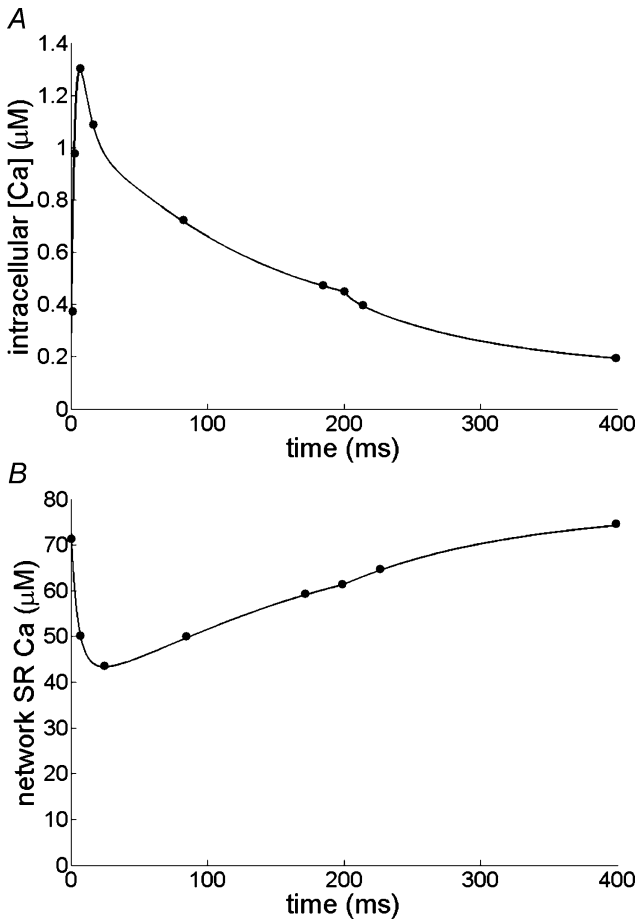

Figure 4. Verification of the Hinch CellML implementation
Intracellular calcium (*A*) and SR calcium concentration changes (*B*) in response to a 200 ms voltage-step depolarization (from −80 to 0 mV) predicted by the CellML model (continuous lines) against digitized data (dots) from Fig. 7 of Hinch *et al.* (2004).

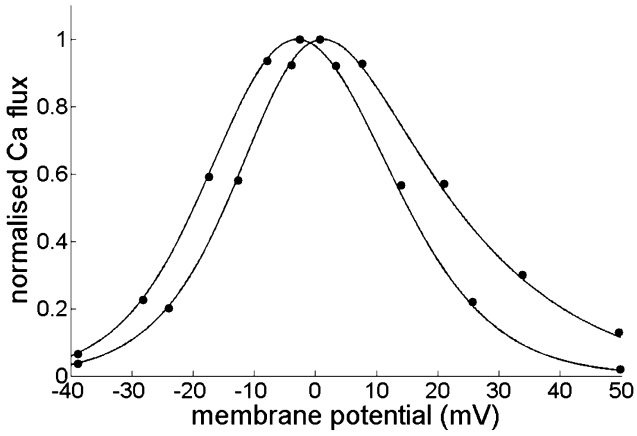

Figure 5. Verification of the Hinch CellML implementation
L-type calcium channel and ryanodine receptor fluxes as a function of membrane potential predicted by the CellML model (continuous lines) against digitized data (dots) from Fig. 8a of Hinch *et al.* (2004). The peak of the ryanodine receptor flux is on the left.

PHN *et al.* model is visualized in Fig. 1*D*, in which the components coloured blue are imported from the Pandit model, red from the Hinch model and green from the Niederer model, while those in black are described in the PHN *et al.* model.

Model compatibility. A common problem associated with ensemble model creation is the issue of compatibility. Some discrepancies between the PHN *et al.* model and its component models are highlighted in Table 2. For example, the Hinch model of calcium dynamics describes all ionic transport in terms of the flux of calcium ions (in mM ms^{-1}) whereas the Pandit model uses whole-cell current (in nA). We chose to encode the PHN *et al.* model with descriptions of whole-cell current represented in microamperes. However, these descriptions of ionic transport need to be of equivalent units in order to calculate the changes in membrane potential in terms of ion concentrations.

In the process of reconciling these differences, we identified three classes of incompatibility, which we will now introduce, before providing examples of how these incompatibility issues were overcome in the PHN *et al.* model.

Unit inconsistencies. The simplest of the three forms of inconsistency refers to the connection of variables (state or otherwise) which differ in the dimension of equivalent units; for example, currents imported from the Pandit model (in nA) and currents in the PHN *et al.* model (in μA). In this case, these differing quantities may be connected directly, because the integration software, PCEnv, automatically converts the dimensions of equivalent units (nA and μA) when passing the variable at this connection.

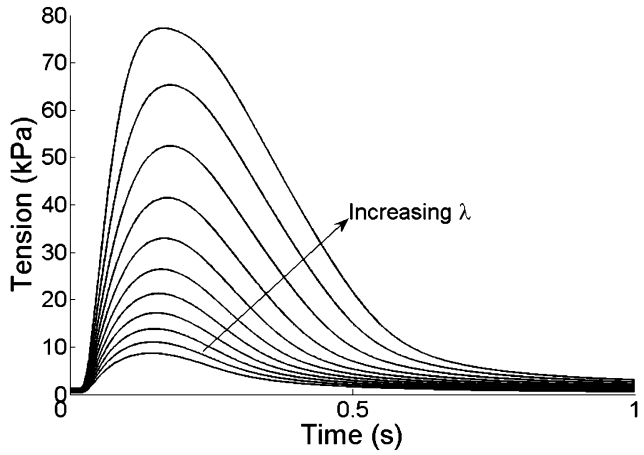

Figure 6. Verification of the Niederer CellML implementation
Tension traces in response to a calcium transient (as prescribed by the data of Janssen *et al.* 2002; their Fig. 1c) for increasing values of λ, as per Niederer *et al.* (Fig. 11a of Niederer *et al.* 2006).

Structural inconsistencies. These refer to the differences in how the biology is embedded in the mathematical equations. For example, both ion fluxes and whole-cell current describe the movement of ions (across the cellular membranes); however, these are not equivalent units which may be converted from one to the other in an automated way. A conversion between these quantities requires additional user-supplied information regarding both the valence of the species in question (in our PHN *et al.* example, this is calcium ions) and the volume of the myocyte.

In order to achieve this conversion in a semi-automated manner, it was necessary to include an additional component in the PHN *et al.* model to serve as an interface between the models, converting the Hinch Ca^{2+} fluxes into compatible cellular currents (μA) using the following equation:

$$I = j \times z \times F \times vol_{\mathrm{myo}} \quad (1)$$

where the current (I) is in microamperes, the flux of calcium ions (j) is in millimolar per milliseconds, z is the valence (in this case +2 for Ca^{2+} ions), F is Faraday's constant (in C mol^{-1}) and vol_{myo} is the volume of the myoplasm in microlitres. However, the dependence of this conversion upon myocyte volume creates additional complications with another form of inconsistency, that is, parameter inconsistency.

Parameter inconsistencies. These refer to the use of different numerical estimations for the same biological quantity; for example, the different values for cell volume used in the imported models (see Table 2). In this particular example, this poses a problem since the conversion of fluxes to currents is dependent upon this parameter and it was thus necessary to reconcile these differing values such that a uniform value was chosen for the combined PHN *et al.* model. Given the significantly lower concentration of cellular Ca^{2+} ($[Ca^{2+}]_i$) than cellular Na^+ ($[Na^+]_i$) and K^+ ($[K^+]_i$) in ventricular myocytes, this quantity ($[Ca^{2+}]_i$) has a higher sensitivity to the volume of the myoplasm, and thus the results of the Hinch model of calcium dynamics are strongly dependent upon the cellular dimensions. Hence, the cell dimensions of Hinch *et al.* (as opposed to those of Pandit *et al.*) were used in the PHN *et al.* model, to ensure an accurate concentration of intracellular Ca^{2+}, a significant regulator of both cellular electrophysiology and contraction. In the current example, the integration of the two models was further aided by the fact that the descriptions of membrane currents presented by Pandit *et al.* were whole-cell currents and thus independent of cell volume.

Parameter adjustment. In the PHN *et al.* model, the following parameters were adjusted (analogous to those

Table 2. Comparison of model parameters and units

	Pandit model	Hinch model	Niederer model	PHN *et al.* model
Currents/fluxes	nA	mM ms^{-1}	n.a.	μA
Volume	9.36×10^{-6} pl	25840 μm^3	n.a.	25.85×10^{-6} μl
Whole-cell capacitance	1.0×10^{-4} μF	1.534×10^{-4} μF	n.a.	1.0×10^{-4} μF
Whole-cell area	n.a.	n.a.	n.a.	1.534×10^{-4} cm^2

listed by Niederer & Smith, 2007). The conductance of the SR leak current ($g_{SR,l}$) was reduced to 1.5918×10^{-5} ms^{-1} (from 1.8951×10^{-5} ms^{-1}) to ensure a steady-state SR Ca^{2+} concentration of 700 μM as per Hinch *et al*. The maximal flux of the Na^+–K^+ pump current ($\bar{I}_{NaK}$) was increased to 0.95×10^{-4} μA (from 0.8×10^{-4} μA) so that the model reproduces the $[Na^+]_i$–frequency response characterized by Despa & Bers (2003) in rat cardiomyocytes, with a steady-state diastolic $[Na^+]_i$ of 10.71 mM at a pacing frequency of 1 Hz. We refer the reader to Niederer & Smith (2007) for further details regarding these parameter adjustments.

Simulation results. To demonstrate the functionality of the model, the PHN *et al.* model was paced at 1 Hz and the resultant action potential, calcium transient and associated tension development are shown in Fig. 7*A*. A 5 s increase

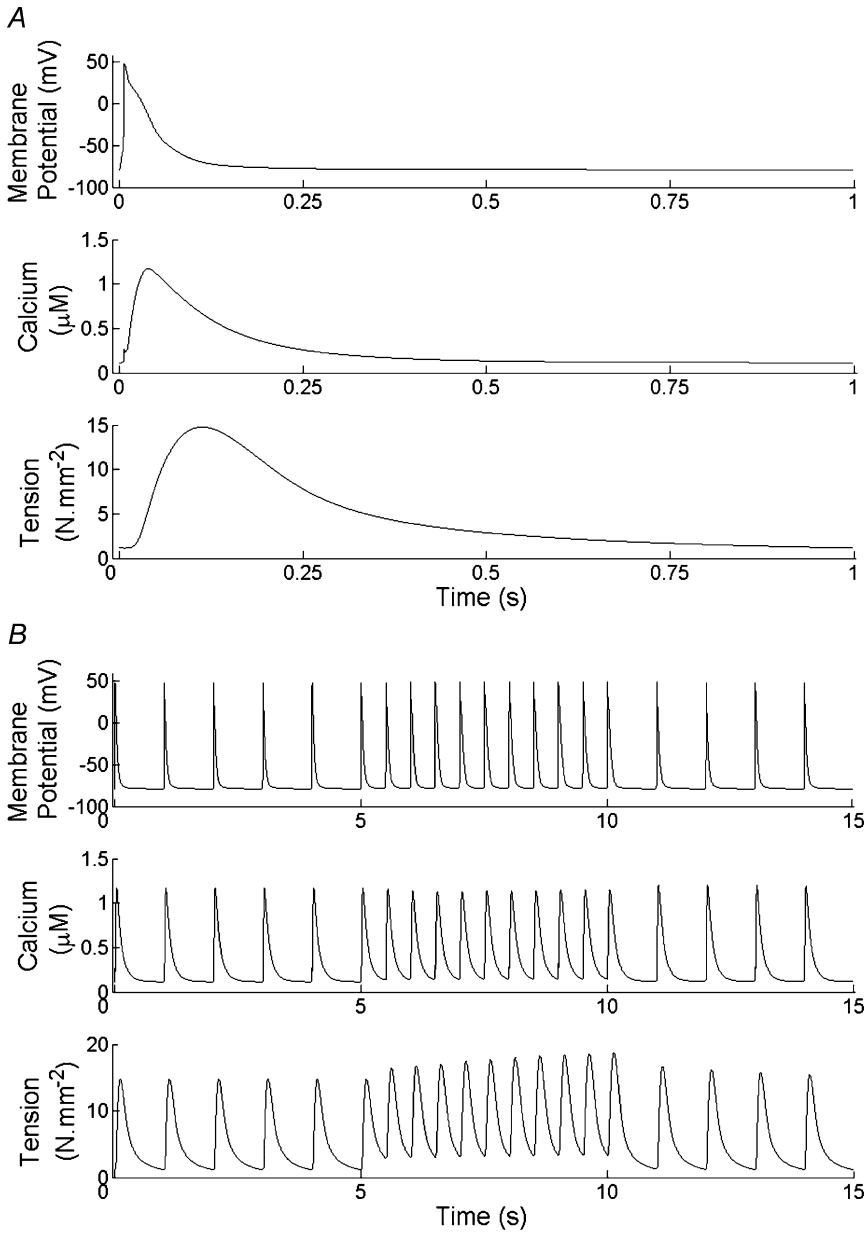

Figure 7. Excitation–contraction traces from the PHN *et al.* model
A, single action potential, associated calcium transient and isometric tension. *B*, action potentials, calcium transient and tension traces associated with a transient frequency increase from 1 to 2 Hz (for 5 s) before returning to the original 1 Hz stimulation frequency.

in stimulation frequency from 1 to 2 Hz results in an increase in both passive and active tension as may be seen in Fig. 7*B*.

Discussion

As discussed in the Introduction, scientific advancement is predicated on the ability to use previous knowledge as a foundation for further research. This process is formalized in computational modelling, where smaller models or parts of models are coupled to create a more complex model. Often, this composite model describes physiological behaviour on a different spatial scale (for example a cell electrophysiology model comprised of components describing properties of transmembrane proteins), but this process is not always achieved in a transparent manner. As a result, it is difficult, at present, for a user to clearly and easily identify how these models relate to each other. Furthermore, the lack of transparency increases the likelihood of the introduction of errors and the possibility of error propagation (Smith *et al.* 2007). Thus, as models of increasing physiological detail are constructed, it is important that we develop a means to reconcile models; to recognize their differences and to analyse their strengths and weaknesses, ideally with the aim of aiding the unambiguous reuse of models or model parts.

A database of validated computational models, from which one may choose and analyse models, is one means with which this may be achieved. A number of model description languages and associated tools have been developed for this purpose [for example, SBML (www.sbml.org), CellML (www.cellml.org), BioPAX (www.biopax.org), JSim (http://physiome.org/jsim/index.html), The Virtual Heart (http://thevirtualheart.org) and Model DB (http://www.ebi.ac.uk/biomodels/)]; however, many of these focus solely on the modelling of biochemical reaction pathways.

CellML is a model description language which may be applied to many forms of biological modelling and whose capabilities were specifically designed to facilitate model reuse (Hedley *et al.* 2001; Cuellar *et al.* 2003). Furthermore, a number of tools exist to support the creation and integration of CellML models, and the online CellML repository (www.cellml.org/models) currently contains 295 mathematical models of biological systems.

In this study, CellML was used to demonstrate the process of model construction by means of reuse of models. We used the three models previously combined by Niederer & Smith (2007). However, these techniques are general, and may be applied to any of the numerous cardiac cell models available in the repository, or indeed, any available model.

The generality of this approach also extends to the methodological issues encountered. The specific details of the issues identified in the construction of the PHN *et al.* model were listed in the previous section. The implications of these issues will now be discussed.

Generally, the conversion of published mathematical models into computer code requires a means with which one may demonstrate the correct implementation of the model. This problem is by no means unique to the approach of this study and is currently being addressed by the CellML community (Le Novere *et al.* 2005; Nickerson & Hunter, 2006). The accepted approach at present is to attempt to reproduce the published results. Unfortunately, the process of reproducing published results is itself fraught with difficulties. Even with an unambiguous description of a model, small discrepancies in the results (stemming from variabilities in the integration algorithms and parameters, initial conditions and degree of steady state) may still arise, suggesting a need for an unambiguous description of these simulation conditions, in addition to that of the mathematics, if users are to understand and reproduce the published results. Furthermore, the publication process itself is imperfect, and published models frequently contain typographical errors (as evidenced above in the Pandit, Hinch and Niederer models). While there is an increasing trend for people to make their model code available, which is a significant step forward, the use of curated repositories where authors to submit a standard-encoded form of the model to a repository concurrent with the published version has the greatest value for the end-users (Cherry & Fenton, 2006). Indeed, model verification postpublication may eventually become redundant if this becomes accepted practice.

However, not only are there challenges associated with the correct implementation of published models in CellML, but there are additional compatibility issues associated with the combination of these models. These issues can be divided into three classes, the simplest of which (unit inconsistencies) may be dealt with automatically by some of the CellML tools. A greater challenge is the reconciliation of structural inconsistencies, whereby the same conceptual quantity is physically represented in two distinct manners; for example, the use of ionic flux *versus* current as the means for characterizing the transport of ions. The incorporation of an interface through which the imported components may interact with the parent model (for example, the 'conversion' component in the PHN *et al.* model) is one solution to the problem; however, the details of that interface will necessarily be specific to the individual problem and thus this process cannot easily be automated. Ideally, as the CellML ontology and associated tools develop, it is conceivable that some of these structural issues may be able to be managed automatically. At present however, specific mechanisms with which to deal with these cases must be developed on a case-by-case basis.

Parameter inconsistencies pose a separate and complicated issue which must be resolved. These discrepancies have important implications for the behaviour of the models, raising the question of how to quantify and account for the resultant numerical differences. It is often difficult to determine which of the differing parameters is more relevant for the current application and thus should be chosen for the coupled model, or whether it is necessary to scale the models according to the differing parameter values. In general, the more transparent the link between a model and the data used for parameterization, the easier it is to assess the applicability of parameters for the coupled model and thus choose between them. An ontology of experimental data (Soldatova & King, 2006) will facilitate this process for the future. For equivalent reasons, general model transparency and a biophysical structure eases the reconciliation of the structural inconsistencies, while also providing a natural interface with which to couple models (Cooling *et al.* 2008).

In the construction of the PHN *et al.* model, we explicitly chose models which are consistent in both species and temperature; however, as highlighted by both Smith *et al.* (2007) and Cherry & Fenton (2006), the issues of consistency (species, temperature, cell type etc.) is one which is paramount for the reuse and coupling of models, and should be addressed by the Physiome Community as a whole. CellML and the associated tools do not themselves have the capacity to address these issues. They do, however, provide mechanisms to make the modelling, and model-coupling, process more transparent to the user and thus support research focused on reducing issues of compatibility and error propogation.

There are two important advantages associated with the construction of models by reusing components encoded in a language such as CellML. The first relates to the ability to combine individual models without first having to recode the model equations. Not only does this reduce the possibility of introducing errors into the model, but it greatly speeds up the process of model creation. Furthermore, it enables subsequent users to get a clear understanding of the structure of the model reuse hierarchy. Users may then individually assess the worth of component models, their parameters and associated experimental data, for their specific application. Secondly, the integration of these models into the same computational framework results in a consistent set of mathematical equations which may be more easily optimized by techniques such as partial evaluation (Cooper & McKeever, 2007) and look-up tables, thus improving the computational efficiency of these models 'at runtime'.

The three component models of the PHN *et al.* model characterize the biology of rat cardiomyocytes with models which demonstrate strong links to the underlying biological processes and their experimental data, resulting in comparatively simple structural and parametric issues to resolve. However, while the individual components may each conform to the experimental data, as for all mathematical models, each component model has a set of limitations, and a simulation range within which it is able to accurately represent the biology of the system. Upon subsequent amalgamation, these individual limitations and simulation ranges may or may not transfer to the new coupled model. For example, the PHN *et al.* model exhibits normal function at slower stimulation frequencies, but the recovery dynamics of the system are such that at significantly higher stimulation frequencies, the behaviour of the system is no longer physiological. The simulation tools aid our investigation into the emergent properties of the model (including the testing of model functionality within, and beyond, the original parameterization range; Cherry & Fenton, 2006) from which we may potentially develop insights into the models and their dynamics, and possibly the biological system itself.

Appendix

Corrected Pandit equations (for definition of terms, see Table A1):

$$\tau_{\mathrm{m}} = \frac{0.00136}{\dfrac{0.32\,(V_{\mathrm{m}} + 47.13)}{1 - \mathrm{e}^{-0.1(V_{\mathrm{m}}+47.13)}} + 0.08\mathrm{e}^{\dfrac{-V_{\mathrm{m}}}{11}}} \tag{A1}$$

$$\tau_h = \begin{cases} 0.0004537\left(1 + \mathrm{e}^{\frac{-(V_{\mathrm{m}}+10.66)}{11.1}}\right) & \text{if} \quad V_{\mathrm{m}} \geq -40\ \mathrm{mV} \\ \dfrac{0.00349}{0.135\mathrm{e}^{\frac{-(V_{\mathrm{m}}+80)}{6.8}} + 3.56\mathrm{e}^{0.079V_{\mathrm{m}}} + 310000\mathrm{e}^{0.35V_{\mathrm{m}}}} & \text{otherwise} \end{cases} \tag{A2}$$

Table A1. Initial conditions for the Pandit endocardial cell model

State Variable	Description	Initial Value
V_m	Membrane potential	−79.565681 mV
m	I_{Na} activation gating variable	0.004825174
h	I_{Na} fast inactivation gating variable	0.641759447
j	I_{Na} slow inactivation gating variable	0.641671606
d	$I_{Ca,L}$ activation gating variable	2.579718 e^{-6}
f_{11}	$I_{Ca,L}$ fast inactivation gating variable	0.999944746
f_{12}	$I_{Ca,L}$ slow inactivation gating variable	0.999944746
Ca_{inact}	Ca^{2+}-inactivation gating variable	0.985762725
r	I_t activation gating variable	0.002362996
s	I_t fast inactivation gating variable	0.87713552
s_{slow}	I_t slow inactivation gating variable	0.410011002
r_{ss}	I_{ss} activation gating variable	0.003126432
s_{ss}	I_{ss} inactivation gating variable	0.2965757
y	I_f inactivation gating variable	0.003051783
$[Na^+]_i$	Intracellular Na^+ concentration	10.10341842 mM
$[K^+]_i$	Intracellular K^+ concentration	137.4335936 mM
$[Ca^{2+}]_i$	Myoplasm Ca^{2+} concentration	1.319981172 e^{-4} mM
$[Ca^{2+}]_{NSR}$	NSR Ca^{2+} concentration	7.75677853 e^{-2} mM
$[Ca^{2+}]_{SS}$	Restricted subspace Ca^{2+} concentration	1.44390143 e^{-4} mM
$[Ca^{2+}]_{JSR}$	JSR Ca^{2+} concentration	7.72445851 e^{-2} mM
P_{C1}	Fraction of channels in state P_{C1}	0.537662547
P_{C2}	Fraction of channels in state P_{O1}	0.46178896
P_{O1}	Fraction of channels in state P_{O2}	0.0005512441
P_{O2}	Fraction of channels in state P_{C2}	3.483581253 e^{-9}
I_{trpn}	Concentration of Ca^{2+}-bound low-affinity troponin sites	0.00816340866 mM
h_{trpn}	Concentration of Ca^{2+}-bound high-affinity troponin sites	0.139650948 mM

$$\tau_{f_{11}} = 0.105e^{-\left(\frac{V_m+45}{12}\right)^2} + \left(\frac{0.04}{1+e^{\frac{-V_m+25}{25}}}\right) + \left(\frac{0.015}{1+e^{\frac{V_m+75}{25}}}\right) + 0.0017 \tag{A3}$$

$$\tau_{f_{12}} = 0.041e^{-\left(\frac{V_m+47}{12}\right)^2} + \left(\frac{0.08}{1+e^{\frac{V_m+55}{-5}}}\right) + \left(\frac{0.015}{1+e^{\frac{V_m+75}{25}}}\right) + 0.0017 \tag{A4}$$

$$i_{K1} = \left(\frac{48}{e^{\frac{V_m+37}{25}} + e^{\frac{V_m+37}{-25}}} + 10\right)\left(\frac{0.001}{1+e^{\frac{V_m-(E_K+76.77)}{-17}}}\right) + \frac{g_{K1}\,(V_m-(E_K+1.73))}{\left(1+e^{\frac{1.613F(V_m-(E_K+1.73))}{RT}}\right)\left(1+e^{\frac{K_o-0.9988}{-0.124}}\right)} \tag{A5}$$

$$I_{NaK} = \bar{I}_{NaK}\left(\frac{1}{1+0.1245e^{\frac{-0.1V_mF}{RT}} + 0.0365\sigma e^{\frac{-V_mF}{RT}}}\right)\left(\frac{K_o}{K_o+K_{m_K}}\right)\left(\frac{1}{1+\left(\frac{K_{m_{Na}}}{Na_i}\right)^{1.5}}\right) \tag{A6}$$

$$\frac{dV_m}{dt} = \frac{-(I_{Na}+I_{CaL}+I_t+I_{SS}+I_f+I_{K1}+I_B+I_{NaK}+I_{NaCa}+I_{CaP}-I_{stim})}{C_m} \tag{A7}$$

where $I_{stim} = 0.6$ nA for 5 ms.

Initial conditions for the Pandit endocardial cell model are listed in Table A1.

Corrected Hinch equations:

$$\frac{d[Ca^{2+}]_i}{dt} = \beta_i(I_{LCC} + I_{RyR} - I_{SERCA} + I_{SR,l} + I_{NCX} - I_{pCa} + I_{CaB} + I_{TRPN}) \tag{A8}$$

The concentration of troponin at resting membrane potential ($[\mathrm{TRPN}]_0$ at a V_0 of −80 mV) was determined analytically by eqn (A9) at a value of 63.6364 μM:

$$[\mathrm{TRPN}]_0 = \frac{k^-_{\mathrm{TRPN}}\,[B]_{\mathrm{TRPN}}}{k^-_{\mathrm{TRPN}} + k^+_{\mathrm{TRPN}}[\mathrm{Ca}^{2+}]_{\mathrm{i},0}} \tag{A9}$$

Similarly, the proportion of CaRU in the combined states at V_0 ($z_{1,0}$, $z_{2,0}$ and $z_{3,0}$) were determined to be 0.9886, 0.00873 and 0.002366 respectively.

Corrected Niederer equation:

$$z_{\max} = \left(\frac{\alpha_0}{\left(\frac{\mathrm{Ca}_{\mathrm{TRPN}_{50}}}{\mathrm{TRPN}_{\mathrm{tot}}}\right)^{n_{\mathrm{Hill}}} - K_2} \right) \frac{1}{\alpha_{r1} + K_1 + \frac{\alpha_0}{\left(\frac{\mathrm{Ca}_{\mathrm{TRPN}_{50}}}{\mathrm{TRPN}_{\mathrm{tot}}}\right)^{n_{\mathrm{Hill}}}}} \tag{A10}$$

References

Cherry E & Fenton F (2006). A tale of two dogs: analyzing two models of canine ventricular electrophysiology. *Am J Physiol Heart Circ Physiol* **292**, H43–H55.

Cooling M, Hunter P & Crampin E (2008). The modularization of models in CellML. *IET Syst Biol* **2**, 73–79.

Cooper J & McKeever S (2007). A model-driven approach to automatic conversion of physical units. *Softw Pract Exp* **38**, 337–359.

Cuellar A, Lloyd C, Nielsen P, Bullivant D, Nickerson D & Hunter P (2003). An overview of CellML 1.1, a biological model description language. *Simulation* **79**, 740–747.

Despa S & Bers D (2003). Na/K pump current and $[\mathrm{Na}]_{\mathrm{i}}$ in rabbit ventricular myocytes: local $[\mathrm{Na}]_{\mathrm{i}}$ depletion and Na buffering. *Biophys J* **84**, 4157–4166.

Hedley W, Nelson M, Bullivant D & Nielsen P (2001). A short introduction to CellML. *Philos Trans R Soc A* **359**, 1073–1089.

Hinch R, Greenstein J, Tanskanen A, Xu L & Winslow R (2004). A simplified local control model of calcium-induced calcium release in cardiac ventricular myocytes. *Biophys J* **87**, 3723–3736.

Hunter P & Borg T (2003). Integration from proteins to organs: the Physiome Project. *Nat Rev Mol Cell Biol* **4**, 237–243.

Hunter P, McCulloch A & ter Keurs H (1998). Modelling the mechanical properties of cardiac muscle. *Progress Biophys Mol Biol* **69**, 289–331.

Janssen P, Stull L & Marban E (2002). Myofilament properties comprise the rate-limiting step for cardiac relaxation at body temperature in the rat. *Am J Physiol Heart Circ Physiol* **282**, H499–H507.

Le Novere N, Finney A, Hucka M, Bhalla U, Campagne F, Collado-Vides J, Crampin E, Halstead M, Klipp E, Mendes P, Nielsen P, Sauro H, Shapiro B, Snoep J, Spence H & Wanner B (2005). Minimum information requested in the annotation of biochemical models (MIRIAM). *Nat Biotechnol* **23**, 1509–1515.

Lloyd C, Halstead M & Nielsen P (2004). CellML: its future, present and past. *Progress Biophys Mol Biol* **85**, 433–450.

Nickerson D & Hunter P (2006). The Noble cardiac ventricular electrophysiology models in CellML. *Progress Biophys Mol Biol* **90**, 346–359.

Niederer S, Hunter P & Smith N (2006). A quantitative analysis of cardiac myocyte relaxation: a simulation study. *Biophys J* **90**, 1697–1722.

Niederer S & Smith N (2007). A mathematical model of the slow force response to stretch in rat ventricular myocytes. *Biophys J* **92**, 4030–4044.

Pandit S, Clark R, Giles W & Demir S (2001). A mathematical model of action potential heterogeneity in adult rat left ventricular myocytes. *Biophys J* **81**, 3029–3051.

Smith N, Crampin E, Niederer S, Bassingthwaighte J & Beard D (2007). Computational biology of cardiac myocytes: proposed standards for the physiome. *J Exp Biol* **210**, 1576–1583.

Soldatova L & King R (2006). An ontology of scientific experiments. *J R Soc Interface* **3**, 795–803.

Acknowledgements

The authors would like to thank Professor Jim Bassingthwaighte for helpful discussions. This work was supported by the Maurice Wilkins Centre and National Institutes of Health grant no. EB005825.